

Chemical stability of metal organic frameworks for applications in drug delivery

Hana Bunzen

Angaben zur Veröffentlichung / Publication details:

Bunzen, Hana. 2021. "Chemical stability of metal organic frameworks for applications in drug delivery." *ChemNanoMat* 7 (9): 998–1007. <https://doi.org/10.1002/cnma.202100226>.

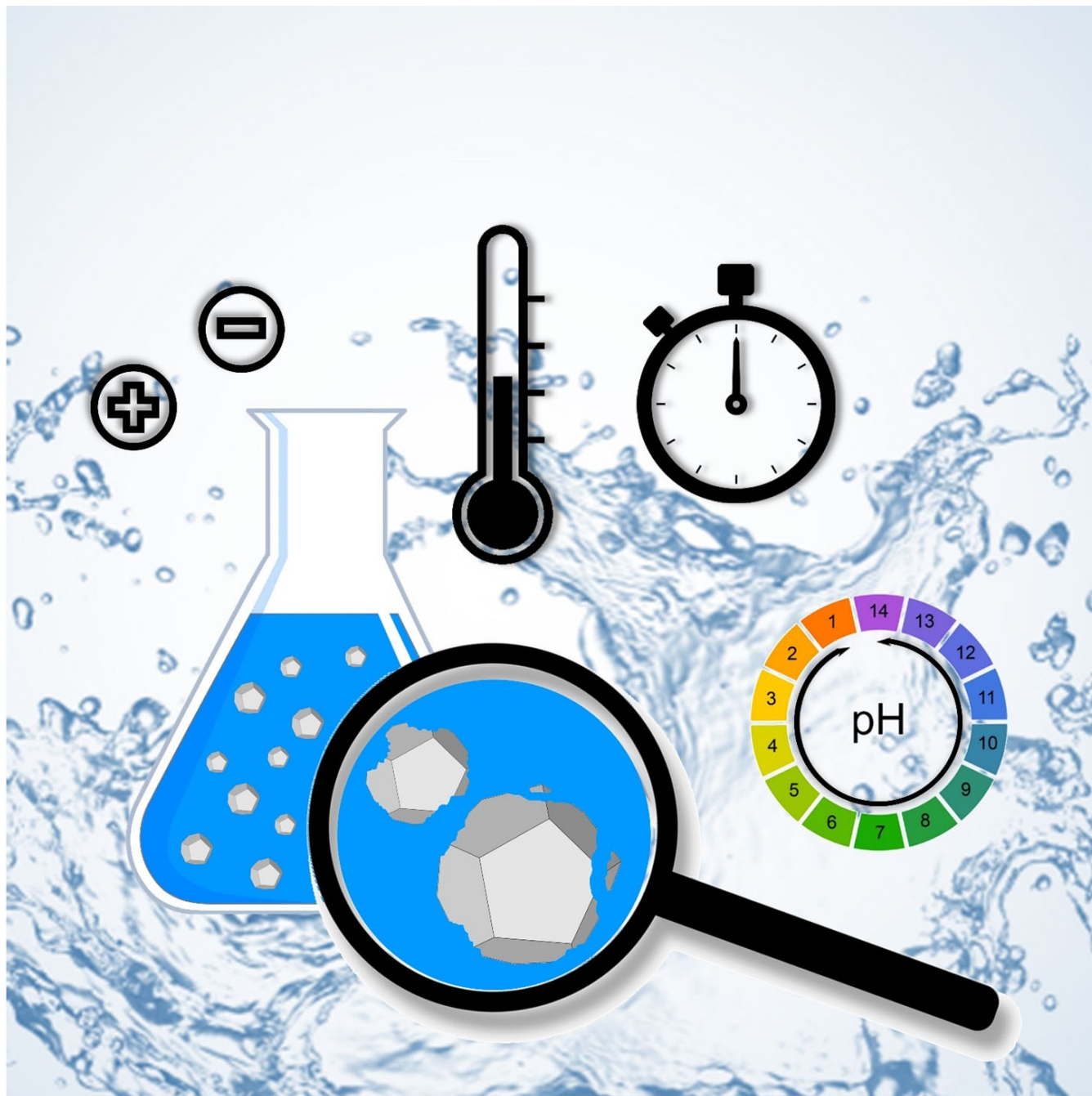
Nutzungsbedingungen / Terms of use:

CC BY 4.0



Chemical Stability of Metal-organic Frameworks for Applications in Drug Delivery

Hana Bunzen*^[a]



Abstract: Structural variety, tunable porosity and opportunities for functionalization make metal-organic frameworks (MOFs) promising materials for applications in medicine as drug delivery systems. In this minireview, an overview of chemical stability of MOF nanocarriers at simulated body conditions is presented. Parameters such as a choice of buffer, pH value, nanoparticle size or surface modification are

discussed, as well as analytical methods and approaches suitable to determine the material stability. Last but not least, examples of tuning and improving the chemical stability of MOF nanoparticles for solution-based drug delivery (oral and intravenous) are presented and examples of MOFs as pH-responsive drug nanocarriers are given.

1. Introduction

Conventional drugs based on small molecules are often distributed at high concentrations in order to reach target tissues at a therapeutic concentration. This can lead to a non-selective biodistribution within the body, which might result in a tissue damage. As an alternative to the traditional approach, using drug delivery systems have been proposed.^[1] Nanoparticles have been suggested as drug delivery platforms to provide controlled drug delivery leading to an increase of efficiency and decrease of side effects. Various materials have been suggested as nanocarriers,^[2–4] including metal-organic frameworks (MOFs),^[5–10] which typically possess a large drug loading capacity (due to the high material porosity), good biocompatibility and opportunities for functionalization.

MOFs are porous coordination polymers constructed from organic ligands and metal-containing nodes.^[11] Due to their structural and functional tunability,^[12,13] they have been considered as promising materials for various applications including gas storage and separation,^[14,15] catalysis,^[16,17] sensing,^[18,19] electrical and proton conduction,^[20,21] but also as nanocarriers in drug delivery.^[5–10] For many of the applications, a high chemical and thermal stability is required and is often a crucial aspect when considering the commercialization of the materials. However, when considering MOFs as drug nanocarriers, a certain material instability can lead to great benefits. For instance, to prevent a nanoparticle accumulation within the body, it would be convenient if the nanocarrier decomposes, when the drug is delivered to the target. The optimal material stability for drug delivery applications strongly depends on the route of administration (oral, intravenous, transdermal, pulmonary, etc.). In this minireview, a chemical stability of MOFs at simulated body conditions for applications in solution-based drug delivery (oral and intravenous) is discussed. Information on other sorts of MOF stability, such as thermal stability and stability in water, was reported in comprehensive reviews previously.^[22–24]

2. The origin of the chemical stability of MOFs

Chemical stability of MOFs refers to their ability to maintain their long-ranged ordered structure in a certain chemical environment. The strength of coordinate bonds is believed to be responsible for the thermodynamic stability of MOFs.^[25] Thus, the stronger the coordinate bonds are, the more stable framework is expected to be formed. The bond strength can be predicted by applying the Pearson's hard and soft acids and bases (HSAB) principle.^[26] According to the HSAB principle, stable MOFs can be formed either by assembly of hard bases (such as carboxylate ligands) with high-valent metal ions [such as Ti(IV), Zr(IV), Al(III), Fe(III) and Cr(III)], or by assembly of soft bases (such as imidazolate, pyrazolate, triazolate and tetrazolate ligands) with soft divalent metal ions [such as Zn(II), Cu(II), Mn(II), etc.]. The metal-ligand bond strengths with a given ligand are positively correlated to charges of the metal cations and negatively correlated to the ionic radius.

When considering the material stability, the operating environment has to be taken into an account too. For instance, a pH value has to be considered. A great effort has been made to explain MOF stability in acids and bases.^[27,28] In an acidic environment, the MOF degradation is mainly caused by competing proton and metal ions to coordinate with the organic ligand. In a basic environment, the major driving force of MOF decomposition is the replacement of organic ligands by hydroxide ions. Therefore, MOFs based on high-valent metal ions and carboxylate ligands are expected to be rather stable in acids, while less resistant to bases. On the other hand, MOFs based on soft divalent metal ions and azolate ligands are expected to be more stable in basic solution and rather unstable in acids. Additionally, the presence of additional cations and ions in the operating environment also influences the stability. For example, phosphate ions in a phosphate buffered saline (PBS) can be seen as ligands, which can replace the organic ligands in MOFs. They can be classified as a hard Lewis base; thus, they are expected to reduce the stability especially of carboxylate-based MOFs constructed from high-valent metal ions. The influence of the buffer choice (with regard to its composition) is discussed in detail in the corresponding paragraph of this minireview.

[a] Dr. H. Bunzen
Chair of Solid State and Materials Chemistry, Institute of Physics
University of Augsburg
Universitaetsstrasse 1, 86159 Augsburg (Germany)
E-mail: hana.bunzen@physik-uni.augsburg.de

© 2021 The Authors. ChemNanoMat published by Wiley-VCH GmbH. This is an open access article under the terms of the Creative Commons Attribution License, which permits use, distribution and reproduction in any medium, provided the original work is properly cited.

3. Analytical methods to determine the chemical stability of MOFs

In a typical stability test, a certain amount of a MOF is dispersed in a certain volume of a selected solution. After a certain period of time, both the liquid and solid phases are analysed. Chemical stability of a MOF is understood as the ability to maintain the long-ranged ordered structure, when exposed to a certain environment.^[25] Therefore, after the material exposure, changes to the material structure has to be assessed. There is a variety of transformations, which may occur and they need to be evaluated by a suitable combination of analytical methods. Generally, there are two main ways of a material degradation to be considered: (i) decomposition to the original building blocks (which can further react with compounds present in the operating environment) and (ii) amorphization.

3.1. Analysis of the solid phase

Powder X-ray diffraction: Recording powder X-ray diffraction (PXRD) patterns is a quick and simple method to study structural changes in a MOF. PXRD patterns of a sample before and after the exposure are measured and compared. The patterns can be identical, reflect slight changes, or show a greater variation. To compare two PXRD patterns, the measurements should be standardized. Falcato et al. proposed to add a known quantity of a crystalline internal standard, such as commercial TiO₂ (anatase).^[29] This approach allows to exclude the possibility that changes in intensity of the diffraction peaks resulted from fluctuations in the mass of the material from sample to sample. The diffraction patterns are recorded and baseline corrected. Then, the peak corresponding to the (101) anatase ($2\theta = 25.3^\circ$) is fitted with a Gaussian curve, and the intensity normalized (Figure 1a).

It should be noted that a PXRD measurement is essentially an incomplete experiment. It may give an impression of stability arising from the retention of the peaks in a PXRD pattern. However, this can be misleading, because even if two PXRD patterns are apparently unchanged, it does not ultimately confirm the stability. For example, an amorphous phase can be formed, while the remaining sample is unchanged, or a part of

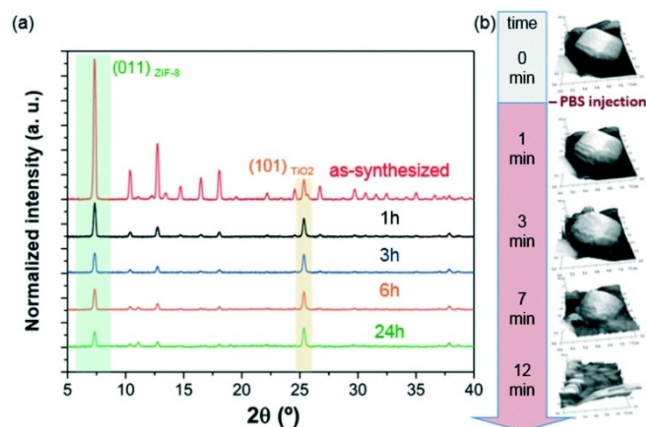


Figure 1. a) PXRD patterns illustrating the structural evolution of ZIF-8 particles before and after the incubation process in PBS, and b) evaluation of the degradation process followed by in situ AFM experiments. Adapted from Ref. [29] with permission from the Royal Society of Chemistry.

the sample can dissolve, while the residual solid remains crystalline. Therefore, a detailed data analysis is necessary to detect a peak broadening, thicker baseline, etc. Other subtle changes, which is not largely captured by the PXRD measurement, are surface defects possibly caused by the treatment. Given all these possibilities, PXRD as a means of determining chemical stability should only be used in a combination with further characterization techniques, including studies of a retention of mass.

Infrared spectroscopy: Infrared (IR) spectroscopy is a suitable technique to determine, if there is a chemical change to the framework (e.g. protonation of the ligand, additional coordination of the solution components to the framework, etc.). The information is then combined with results from other methods to assess, if the structure has changed. Falcato et al. used IR spectroscopy to show changes in ZIF-8 after exposing it to PBS.^[29] They reported on a progressive decrease in the peak intensity of vibration modes related to 2-methylimidazolate ligand and of the band attributed to the Zn–N stretching mode. The data suggested that the degradation process of ZIF-8 involved the release of the ligand with a change in the coordination environment of the Zn(II) ions. Moreover, new vibrational mode were detected at 1160–900 cm^{−1} and 660–530 cm^{−1} with increasing intensity over time. These bands were assigned to the antisymmetric stretching and bending mode of PO₄^{3−} groups, respectively, indicating that the phosphate ions from the buffer solution reacted with released zinc ions to form zinc phosphates as a degradation product.

Electron microscopy: To determine changes in a particle size or morphology, electron microscopy is often employed. The methods include atomic force microscopy (AFM), scanning electron microscopy (SEM) and transmission electron microscopy (TEM). For instance, AFM images of ZIF-8 particles were taken to follow etching of the external surface of the particles (Figure 1b).^[29] The micrographs showed a faster degradation of nanoparticles in comparison to microsized particles as a result of the larger surface area of the nanoparticles being exposed to

Hana Bunzen is an assistant professor at the Chair of Solid State and Materials Chemistry at the University of Augsburg, Germany. She completed her master degree in chemistry at the University of Chemistry and Technology in Prague, Czechia, and earned her PhD in organic chemistry at the University of Jyväskylä in Finland. Since 2018 she leads a junior research group focused on functional hybrid materials including materials for drug delivery.



PBS. Moreover, electron microscopes often provide the possibility to performed energy-dispersive X-ray spectroscopy (EDX), which can be used for an elemental analysis of the solid. Similarly, Gassensmith et al. studied the changes in morphology of 1 μm large ZIF-8 crystals exposed to various buffers and cell media by time resolved SEM microscopy combined with EDX.^[30]

3.2. Analysis of the liquid phase

Mass balance: Checking if a MOF is 'dissolving' should be one of the first properties to study, when determining the material chemical stability. This can involve weighing the sample pre- and post- stability tests or monitoring the parent solution. Since it is rather difficult to isolate the material quantitatively (especially if well-dispersible nanoparticles of a size of tens of nanometres are used) and make sure that there are no components or solvent molecules of the operating environment trapped in the pores, an indirect method based on monitoring the possibly released MOF components into the solution is usually preferred. If the products of the material degradation are soluble in the tested environment, their amount can be determined and used to quantify the degradation process. However, if that it is not the case and the components are insoluble (as some organic ligands are in aqueous solutions) or react with the buffer medium to form insoluble compounds (i.e. released metal ions to form inorganic salts with the anions present in the operating environment), other methods of a stability determination have to be used. Keeping this in mind, the solubility of the MOF components in the selected operating environment should be tested before the actual MOF stability tests are carried out. The amount of an organic ligand can be determined by various methods (depending on the ligand properties) including high performance liquid chromatography (HPLC), ultraviolet-visible light (UV-VIS) spectroscopy, gas chromatography coupled with mass spectrometry (GC-MS), or nuclear magnetic resonance (NMR) spectroscopy. The amount of the released metal ions is usually determined by inductively coupled plasma mass spectrometry (ICP-MS), or inductively coupled plasma optical emission spectrometry (ICP-OES).

Forgan et al. determined the amount of the ligand (terephthalic acid) released from UiO-66 in PBS by UV-Vis spectroscopy. At different times, 1 mL of liquid was taken and replaced with 1 mL of fresh PBS. The absorbance of the removed solution was measured and by employing a calibration curve, the amount of the released ligand was determined.^[31] In another work, Demel et al. used HPLC (for the ligand determination) and ICP-MS (for the metal determination) to monitor degradation of the UiO-66 in various buffers and in water.^[32] Horcajada et al. also used HPLC as an analytical method to determine the amount of ligand (trimesic acid) released from MIL-100(Fe) into various media.^[33,34] Falcaro et al. determined the amount of the ligand (2-methylimidazole) released from ZIF-8 into PBS by carrying out GC-MS measurements.^[29] Gassensmith et al. followed the Zn-release from ZIF-8 by ICP-MS.^[30]

It should be noted that one method cannot do it all and that a suitable combination of analytical methods has to be

employed to determine the material stability. As a minimal requirement to assess the material stability, PXRD, IR spectroscopy and one microscopy technique should be used to analyse the solid, and at least one method to quantify the amount of the ligand and metal ions released into the solution. To describe and understand the degradation process in detail, additional measurements are usually needed, such as small-angle X-ray scattering, pair distribution function analysis, computation modelling, etc.

4. Experimental set-up and influence of experimental parameters

Just as there are different methods available for assessing the materials stability, there are also different parameters to be consider, when carrying out the stability tests. Besides the material itself (i.e. internal factors such as the type of the metal-ligand coordinate bond, coordination geometry, etc.), the experimental set-up (i.e. external factors including the choice of the operating environment, temperature, concentration, time, etc.) effects the outcome of the stability tests too.

In a typical stability test, a defined amount of the MOF is dispersed in a defined volume of a selected solution. After dispersing MOF nanoparticles in the solution (either in a closable container or dialysis bag), the suspension is kept at a defined temperature – usually 37 °C to simulate the body temperature. Sometimes the samples are stirred or shaken (to mimic the bloodstream), sometimes not. After a certain period of time, the liquid and solid phases are analysed (by a combination of methods described in the previous chapter). When reporting on results of chemical stability, the exposure conditions (i.e. type of the operating environment and its strength, temperature, concentration, time and the experimental set-up in general) need to be specified, because they effect the results as demonstrated on the examples given in the following paragraphs.

4.1. Influence of time

The material chemical stability as a function of time is one of the most important factors to study. The optimal required stability depends on the application and route of administration intended. For some applications, a long-term stability over several days is desired, for other applications, stability over few hours might be sufficient. As a benchmark, 24 hours should be adopted as the initial treatment time, with subsequent treatment times depending on the initial result.

4.2. Operating environment

The operating environment (external factor) and the MOF structure (internal factor; described in the second chapter) are the two major aspects that affect the chemical stability of the

material. Depending on the desired application of the nano-carrier, different operating environments might be better suited. In the simplest experiment, water is used as a solution. However, water does not simulate the body conditions well. Therefore, solutions containing various ions and molecules (including proteins) at concentrations found in the body are usually preferred.^[35] Additionally, to maintain the pH value, these solutions are most of the time buffered.^[36] An overview on common solutions used to simulate body conditions is given in Table 1.

PBS is one of the most commonly used buffer solutions for determining MOF stability, because its ion concentration and osmolarity mimic well the conditions found in the body. It has been shown that the phosphate ions presented in the solution attacked metal ions or clusters of MOFs resulting in a ligand substitution followed by MOF degradation. Fairen-Jimenez et al.

studied the degradation of Zr(IV)-carboxylate MOFs in PBS and in water.^[37] As expected, phosphate groups (PO_4^{3-}) present in the PBS buffer attacked the metal clusters of the MOFs, substituting the carboxylic ligands (as observed by FTIR measurements), and finally disrupting the crystalline MOF structure (as observed by PXRD measurements). In another study, Falcaro et al. reported on the stability of ZIF-8 particles exposed to PBS. They showed that the phosphate ions reacted with released zinc ions to form zinc phosphate.^[29]

Demel et al. reported on a comprehensive study comparing the stability of UiO-66 in different buffers, namely 2-amino-2-(hydroxymethyl)-1,3-propanediol (TRIS), 4-(2-hydroxyethyl) piperazine-1-ethane sulfonic acid (HEPES), N-ethylmorpholine (NEM) and phosphate buffer (PB).^[32] The stability of the material was assessed by monitoring the release of the terephthalate ligand (determined by HPLC, Figure 2) and zirconium ions (determined by ICP-MS). The authors showed that the chemical nature of the buffer media played a decisive role in the MOF stability. Buffers containing large amount of saline forms were found to be more destructive (Figure 2). The HEPES and TRIS buffers were found to be relatively benign, whereas NEM and PB showed a rapid degradation of the UiO-66 framework.

Similarly, Gassensmith et al. reported on the stability of ZIF-8 exposed to various media, including common buffers (PB, HEPES, TRIS, bicarbonate buffer), cell media and serum.^[30] They studied not only the changes in the MOF structure, morphology and crystallinity, but also the influence of the operating environment on the release of cargo represented by green fluorescent protein biomimetically mineralized within ZIF-8. It was reported that buffers containing phosphate and bicarbonate influenced the morphology and composition of ZIF-8, but they did not cause cargo to leak out, whereas, serum dissolved ZIF-8 resulting in a premature cargo release.

Horcjada et al. studied the degradation of MIL-100(Fe) in water and in PBS with and without bovine serum albumin (BSA).^[33] The release of the organic ligand was followed by HPLC (Figure 3a). The results suggested that the MOF nanoparticles were stable in water with a very low amount of the ligand released after 24 h (2.5 ± 0.4 wt%), but much less stable in PBS exhibiting a faster initial degradation of 22.3 ± 2.1 wt% during the first 6 h and a smoother degradation profile unto 29.9 ± 2.1 wt% after 24 h. The addition of BSA to the PBS

Table 1. Overview of buffer solutions ^[36] and simulated fluids ^[35] often used in MOF stability tests.		
Abbrev.	Name	Comment
TRIS	Tris(hydroxymethyl)-aminomethane	Buffer range: 7.4–8.4 $\text{pK}_a = 7.91$ (37 °C)
HEPES	2-[4-(2-Hydroxyethyl)-piperazin-1-yl]ethanesulfonic acid	Buffer range: 6.8–7.8 $\text{pK}_a = 7.33$ (35 °C)
PB	Phosphate buffer	Composition: Na_2HPO_4 , KH_2PO_4 Buffer range: 6.3–7.3 $\text{pK}_a = 6.78$ (35 °C)
PBS	Phosphate buffered saline	Composition: Na_2HPO_4 , KH_2PO_4 , KCl, NaCl pH 7.4 (pH can be adjusted using HCl or NaOH)
SBF	Simulated body fluid	Composition: NaCl, NaHCO_3 , KCl, K_2HPO_4 , MgCl_2 , HCl, CaCl_2 , Na_2SO_4 , tris(hydroxymethyl)aminomethane pH 7.4; used to simulate human blood plasma.
SIF	Simulated intestinal fluid	Composition: sodium taurocholate, lecithin, maleic acid, NaOH, NaCl pH 6.5; used to simulate preprandial conditions in the upper small intestine.
SGF	Simulated gastric fluid	Composition: sodium taurocholate, lecithin, pepsin, NaCl pH 1.6; used to simulate condi- tions in the stomach (fasted-state).

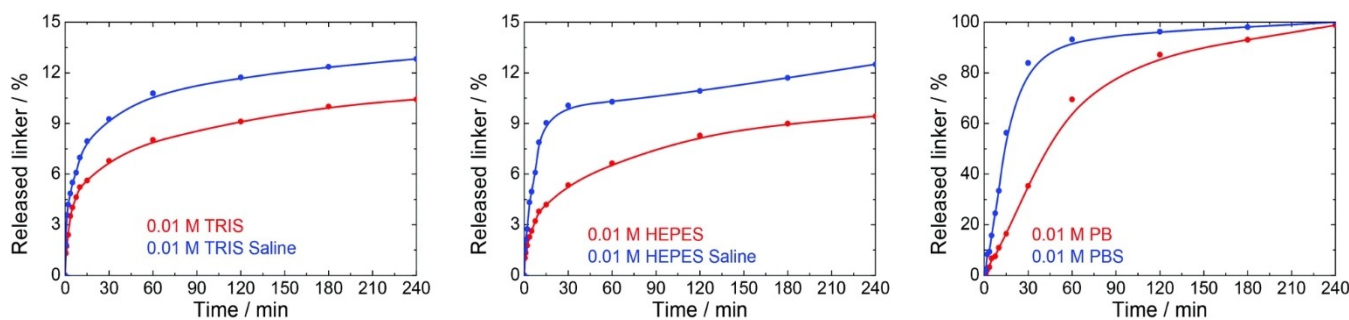


Figure 2. Release of the ligand (terephthalic acid) from UiO-66 in 0.01 M TRIS, HEPES and PB buffers at pH 7.5 and in their saline forms containing 0.15 M NaCl. Reproduced from Ref. [32] with permission from the Royal Society of Chemistry.

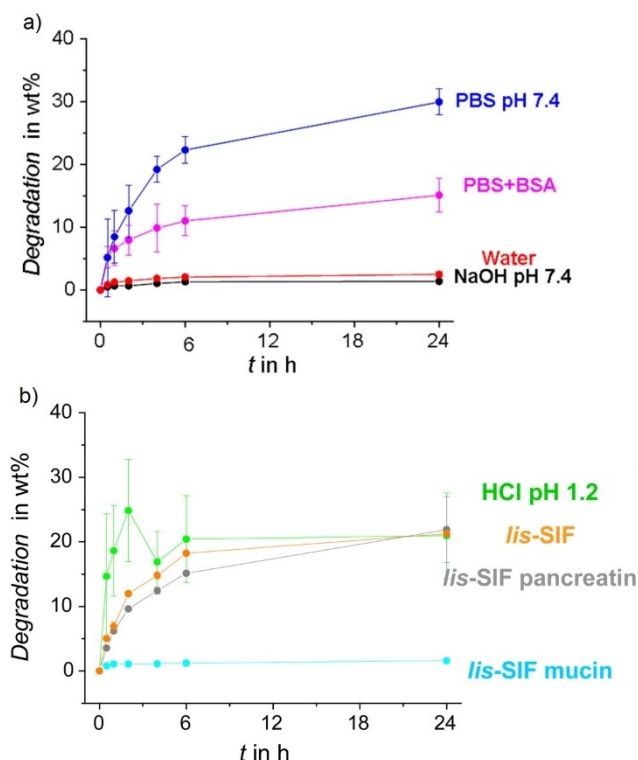


Figure 3. Degradation kinetics of MIL-100(Fe) nanoparticles at 37 °C as a function of time in different physiological media: (a) water, 0.3 mM NaOH pH 7.4, PBS pH 7.4, and PBS + BSA, and (b) HCl pH 1.2, lis-SIF, lis-SIF supplemented with pancreatin, and lis-SIF supplemented with mucine. Degradation is represented as the wt % of the linker released from the MOF into the medium determined by HPLC. Adapted with permission from Ref. [33]. Copyright (2014) American Chemical Society.

medium (5.4% w/v) resulted in a reduction of the kinetics of degradation (15.1 ± 2.7 wt% after 24 h). This effect was attributed to the presence of the BSA protein corona around the nanoparticles, that could hamper the diffusion of the phosphates inside the MOF structure and hence the progressive replacement of the ligands by phosphates. To mimic the conditions of an oral distribution, the stability of MIL-100(Fe) was further studied in simulated intestinal fluid (SIF) and HCl (Figure 3b). Interestingly, the 24 h degradation of the particles in gastric (21.0 ± 6.6 wt% in HCl, pH 1.2) and intestinal (18.2 ± 0.3 wt% in SIF) conditions was similar to that in PBS (29.9 ± 2.1 wt%). Similarly as in PBS, the presence of phosphates in intestinal conditions induced a progressive replacement of the carboxylic ligands in the structure and thus the disassembling of the nanoparticles. At pH 1.2, the ligands were protonated, which led to the structure degradation. For a better understanding of the interaction of MIL-100(Fe) with enzymes secreted by the pancreas in the intestinal tract, the authors carried out additional stability studies in lis-SIF supplemented with pancreatin and mucin. Mucin was found to coat the nanoparticles to form a protective layer, which prevented the nanoparticles from a contact with the surrounding medium, which resulted in a significantly lower ligand release (1.6 ± 0.1 wt%).

It should be noted that not only the type but also the concentration (strength) of the operating environment influence the material stability. For instance, Demel et al. demonstrated that the stability of UiO-66 in TRIS, HEPES, PB and NEM significantly varied based on the buffer concentration varying from 0.01 to 1.0 mol/L.^[32] Therefore, it is important that the buffer concentration is always mentioned when reporting on the stability results.

4.3. Temperature

After dispersing MOF nanoparticles in the selected solution, the suspension is kept at a defined temperature – usually 37 °C to simulate the body temperature. However, there are also some studies reported, which were carried out at 25 °C or at a not precisely defined “room temperature”. Since it has been shown by Demel et al. on an example of UiO-66 (studied at 25 and 37 °C in PB, TRIS and HEPES buffers),^[32] that the chemical stability depends on the temperature used in the experiments, to mimic the body conditions, temperature of 37 °C should be preferred in studies dealing with chemical stability of MOFs for applications in nanomedicine. Moreover, it might be useful to also study the material chemical stability at higher temperature (e.g. around 42 °C) to unlock the potential use of the material in temperature triggered drug delivery and hyperthermia therapy.^[38] Qian et al. reported on a temperature triggered drug release of methotrexate from a Zn-TBDA MOF (TBDA, 4'-(1H-tetrazol-5-yl)-[1,1'-biphenyl]-3,5-dicarboxylic acid).^[39] They showed that at 37 °C after 48 h at pH 7.4, 43% of methotrexate was released, whereas at 42 °C, it was almost 80%. However, it was not shown, if it was caused by a different material stability at these two temperatures.

4.4. Concentration

In a typical stability test a defined amount of the MOF is dispersed at a defined volume of a selected solution. The used concentration quite varies, most of the time being between 0.1 mg of a MOF in 1 mL of the solution to 1 mg/mL. Systematic studies, which would report on the influence of the different experimental concentrations on the material stability (and if there is any) are unfortunately missing. Optimally, the same concentration, at which the nanocarrier is intended to be used in *in vivo* experiments, should be also used in the stability studies.

4.5. Particle size

Particle size is an important property of a nanocarrier. Depending on the intended application and the route of administration, different MOF particle sizes are preferred.^[40] For instance, nanoparticles smaller than 200 nm are believed to be capable of passive targeting in cancer therapy due to the enhanced permeability and retention effect.^[41] It should be noted that the

particle size does not decide only on the fate of nanoparticles in the body, but also affects the material chemical stability. For instance, Falcaro et al. presented a study of ZIF-8 particles of two different particle sizes (2 μm and 250 nm) exposed to PBS.^[29] They demonstrated that the kinetics of the decomposition depended on the particles size and was faster for smaller particles. Therefore, prior the experiments, the material particle size should be determined and reported in every study.

4.6. pH value

A pH value is one of the most discussed parameters in the stability studies of nanocarriers for cancer treatment. Due to the metabolism of cancer cells, the environment of cancer tissues is slightly more acidic in comparison to the blood and normal tissues (pH 7.4).^[42] Therefore, if a nanocarrier, which is stable at pH 7.4, but decomposes at slightly acidic conditions, is used, not only that the nanoparticle accumulation within the body is prevented, but also a site-specific drug release can be achieved. This approach has been also suggested for drug delivery with MOF nanoparticles in cancer therapy.^[8,9] Therefore, if an application of MOFs in cancer treatment is intended, then the material stability should be studied not only at pH 7.4, but also at slightly acidic conditions. In most of such studies, a pH value between 5.5–6.5 is used. On the other hand, if an oral administration is intended, such MOFs should be stable at acidic conditions (to protect the drug from gastric acid), but decompose in the intestine to release the drug, which is then absorbed. There are only several studies demonstrating the chemical stability of “empty” MOFs at different pH values. These examples include ZIF-8,^[29] UiO-66,^[31,32] or MIL-100(Fe).^[33] Usually, most of such studies are carried out with MOF nanoparticles loaded with drug molecules and it is often concluded that the different drug release at different pH values is a result of the different material stability at the pH values. However, without studying also the ‘empty’ MOFs, such conclusions can be misleading, because also other effects (e.g. different interaction between the framework and drug molecules at different pH values as a result of framework or drug protonation, etc.) can be involved and effect the drug release kinetics. In the following overview, examples, where the drug release was triggered by the different material stability at the different pH values, are primary given.

pH-responsive release from Zn-MOFs: Several Zn-MOFs have been reported as pH-responsive nanocarriers for drug delivery.^[6,8] A typical example being ZIF-8, which have been reviewed recently.^[43,44] For instance, ZIF-8 has been reported as a pH-responsive carrier of anticancer drugs such as doxorubicin,^[45,46] camptothecin,^[47] 5-fluorouracil,^[48] or arsenic trioxide.^[49,50] In all these examples, the drug release was faster at acidic pH than at pH 7.4.

Qian et al. reported on a MOF Zn-TBDA (TBDA, 4'-(1H-tetrazol-5-yl)-[1,1'-biphenyl]-3,5-dicarboxylic acid), which they loaded with methotrexate. They showed that in PBS at 37 °C, only 43% of the drug was released at pH 7.4 over 48 h, whereas at pH 6.5 it was 61% due to the influence of the acidic

environment on the MOF structure.^[39] In another work, MOFs Zn-MOF-74^[51] and MFU-4l^[52] were used as pH-responsive nanocarriers of arsenic trioxide. In both cases, it was shown that the drug release was faster at pH 6.0 than at pH 7.4 as a result of the accelerated material decomposition at the more acidic environment.

pH-responsive release from Fe-MOFs: MIL-100(Fe) is a typical example of an iron MOF often proposed for drug delivery due to its biocompatibility.^[33] Based on the HSAB concept,^[26] Fe(III)-carboxylate MOFs are expected to be more stable in acids than in bases (see the second chapter for an explanation). However, Fan et al. reported on a core-shell structure polypyrrole@MIL-100(Fe) loaded with doxorubicin, which exhibited a pH-responsive drug release in PBS at 37 °C.^[53] Around 42.7% of doxorubicin was released after 24 h in the neutral PBS (pH 7.4), whereas 82.7% was released at pH 5.0. In acidic conditions the NH_2 -group of doxorubicin got protonated, which weakened the electrostatic interactions between the drug and MOF, and thus facilitated the drug release.

Huang et al. reported on an Fe-MOF composed of Fe(II) ions and 1,1'-(1,4-butanediyl)bis(imidazole) loaded with doxorubicin.^[54] Due to the sensitivity of the Fe(II)-imidazolate coordinate bonds to acidic environment, the drug was released faster at pH 5.5 than at pH 7.4. The rapid decomposition of the nanocarrier (and thus the drug release) at low pH could be slowed down by coating the MOF surface with a layer of silica.

pH-responsive release from Zr-MOFs: Based on the HSAB concept,^[26] Zr(IV)-carboxylate MOFs are expected to be rather stable in acids, while less resistant to bases (see the second chapter for an explanation). However, there are several reports in literature showing an accelerated drug release from Zr(IV)-carboxylate MOFs in an acidic environment. However, in these examples the triggered drug release is not due to increase framework instability at lower pH values, but rather due to the drug-framework interactions being affected by the environment. Shi et al. reported on a pH-responsive behaviour of UiO-66 for delivery of alendronate.^[55] The drug was anchored to the Zr–O clusters. The release of the drug, tested in PBS buffer at 37 °C, was faster at pH 5.5 (59%) than at pH 7.4 (43%). This was possible because alendronate was protonated in the acidic environment, which weakened the interaction between the drug and the Zr–O clusters in UiO-66. However, because UiO-66 has a lower degradation rate under acidic conditions than under neutral and basic conditions,^[31,32] after 108 h, the amount of the drug released at pH 7.4 was higher than that released at pH 5.5. Similarly, Qian et al. reported on a cationic MOF (ZJU-101) built from zirconium and 2,2'-bipyridine-5,5'-dicarboxylate for the delivery of the anionic drug diclofenac sodium.^[56] The release of the drug was more rapid in PBS at pH 5.4 than at pH 7.4, because ion exchange between the drug and anions occurred more frequently in acidic environments, which discharged the coulombic interaction between the positively charged ZJU-101 and negatively charged drug.

On the other hand, due to the higher stability of Zr(IV)-carboxylate MOFs in acidic conditions, Zr-MOFs have been tested as drug nanocarriers for oral delivery. Qian et al. suggested that a porphyrin-based Zr-MOF (PCN-221) could pass

the stomach and gastrointestinal tract and safely deliver the cargo to body parts with higher pH levels.^[57] However, the experiments were demonstrated only in-vitro on PC12 rat cells. They loaded PCN-221 with methotrexate and studied the drug release in PBS at 37 °C at pH 7.4 (pH close to the intestinal pH) and at pH 2.0 (pH close to the pH of the stomach). After 72 h, only around 40% of the loaded drug was released at pH 2.0, but 100% at pH 7.4. In another work, Farha et al. reported on an immobilization of insulin in an acid stable MOF, NU-1000.^[58] Due to the protective effect from NU-1000, insulin was stable even upon exposure to stomach acid (pH 1.5–3.5) and pepsin. Moreover, 40 wt% of insulin could be released from the host framework under simulated physiological conditions (pH 7.0) (Figure 4).

5. Tuning MOF stability

In general, two main approaches have been adopted to improve the chemical stability of MOFs: (i) de novo synthesis of MOFs, and (ii) improving stability of existing MOFs.

5.1. De novo synthesis

The de novo synthesis widely relies on the HSAB principle.^[26] Carboxylate ligands and high-valent metals are expected to form chemically stable MOFs. Additionally, also phosphonate and phenolate-based ligands are expected to form stable frameworks with high-valent metals, although they have not been widely used in medicinal applications yet. Apart from high-valent metal ions, soft low-valent metal ions can also construct stable frameworks, if they are combined with soft ligands such as N-containing ligands (imidazoles, pyrazoles, triazoles, and tetrazoles). When designing new MOFs for medicinal applications, due to the potential material toxicity, the components selection is rather limited. For this reason, MOFs comprising iron and zinc ions, and no or low toxic ligands are mainly used. Besides the strength of the coordinate bond, which determines the thermodynamic stability, also kinetic factors such as framework rigidity has to be considered. Dense

and rigid structures are typically more stable. For instance, when the stability of isorecticular MOFs UiO-66 and UiO-67 was investigated, decreased stability with an increase in ligand length was observed.^[59]

5.2. Tuning stability of existing MOFs

Coating the nanoparticle surface by polymers has been proposed as an efficient method to improve the chemical stability of MOFs.^[60,61] There are many examples of drug nanocarriers, which have been coated by polyethylene glycol (PEG) to improve their stability (both chemical and colloidal).^[62] For example, Forgan et al. coated UiO-66 nanoparticles with PEG550 and PEG2000.^[31] They showed that the polymer coating enhanced the stability of the nanoparticles in PBS (Figure 5). Similarly, Horcajada et al. reported on stability of MIL-100(Fe). They showed that the degradation could be slowed down by coating the nanoparticles with chitosan.^[34]

6. Summary and Outlook

Chemical stability of MOF nanoparticles depends on many different parameters including the experimental set-up. Therefore, when discussing and presenting the results, the exposure conditions (i.e. type of the operating environment and its strength, temperature, concentration, time, particle size, etc.) have to be specified. As analytical methods, PXRD, IR spectroscopy and one microscopy technique should be used to analyse the solid, and at least one method of quantifying the amount of the ligand and metal ions released into the solution.

Although, we have already learnt a lot about MOF stability with regard to their potential applications in nanomedicine as

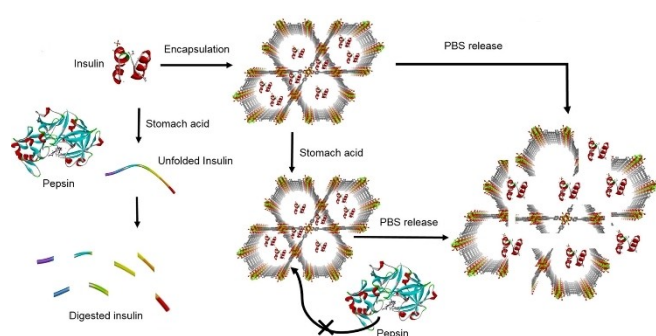


Figure 4. Schematic representation of exposure of free insulin and insulin@-NU-1000 to stomach acid. Adapted with permission from Ref. [58]. Copyright (2018) American Chemical Society.

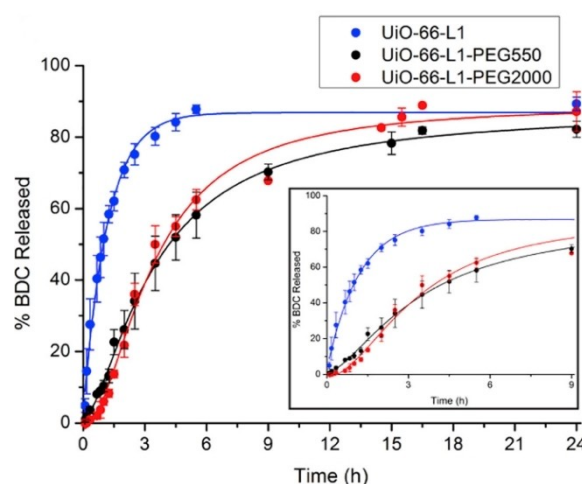


Figure 5. Degradation profiles of UiO-66, UiO-66-PEG550, and UiO-66-PEG2000 in PBS (pH 7.4) determined by UV-Vis spectroscopy. Error bars denote standard deviations from triplicate experiments. Adapted from Ref. [31], Copyright (2017), with permission from Elsevier.

drug delivery systems. There are still some remaining issues to be considered and addressed:

- 1) More systematic studies, which use a combination of analytical methods, need to be carried out. For instance, it is not sufficient to carry out drug release studies and conclude that the different release at different pH values is a result of different material degradation at these pH values, without studying the material stability without the drug, because there are also other factors, which can contribute to the pH-triggered drug release than just the material stability.
- 2) Stability studies should be carried out in simulated conditions, which are as close as possible to in vivo conditions. This includes a suitable selection of the operating environment, concentration, temperature, etc. as well as suitable particle surface modification.
- 3) Although, there are reports on stability studies of MOF nanoparticles carried out at simulated body conditions, studies linking and translating the results to studies carried out in vivo are scarce. However, such studies are needed and are crucial for an effective translation of MOF nanoparticles from bench to bed.
- 4) There is also a lack of clarity around the meaning of MOF stability. Does stability refer to the structure retention or function retention, or both? In this review, stability was discussed as an ability to retain the structure. However, there is no clear view concerning the remaining function upon the exposure. It has been shown that MOFs, which lost their crystallinity, can be efficient in drug delivery and sometimes even exhibit better results than the related crystalline equivalents.^[37,63]
- 5) Last but not least, it should be noted that in the minireview, examples of solution-based drug delivery (oral or intravenous) were primarily discussed and that for other routes of administration (transdermal, pulmonary, etc.), different experimental set-ups and requirements of the material stability are expected. Additionally, the stability in formulation, processing, pelletisation, etc. should be also considered.

However, despite the mentioned issues, there is no doubt that MOFs still remain one of the most promising materials for drug delivery.

Acknowledgements

The author is grateful to the SPP 1928, COORNETs supported by the German Research Foundation. Open access funding enabled and organized by Projekt DEAL.

Conflict of Interest

The authors declare no conflict of interest.

Keywords: metal-organic framework • stability • drug delivery • nanomedicine • nanoparticles

- [1] N. Wang, X. Cheng, N. Li, H. Wang, H. Chen, *Adv. Healthcare Mater.* **2019**, *8*, 1801002.
- [2] M. J. Mitchell, M. M. Billingsley, R. M. Haley, M. E. Wechsler, N. A. Peppas, R. Langer, *Nat. Rev. Drug Discovery* **2021**, *20*, 101–124.
- [3] W. Park, K. Na, *Wiley Interdiscip. Rev. Nanomed. Nanobiotechnol.* **2015**, *7*, 494–508.
- [4] W. H. De Jong, P. J. A. Borm, *Int. J. Nanomed.* **2008**, *3*, 133–149.
- [5] J. W. M. Osterrieth, D. Fairen-Jimenez, *Biotechnol. J.* **2021**, *16*, 2000005.
- [6] J. Yang, Y.-W. Yang, *Small* **2020**, *16*, 1906846.
- [7] L. Wang, M. Zheng, Z. Xie, *J. Mater. Chem. B* **2018**, *6*, 707–717.
- [8] W. Cai, J. Wang, C. Chu, W. Chen, C. Wu, G. Liu, *Adv. Sci.* **2019**, *6*, 1801526.
- [9] M.-X. Wu, Y.-W. Yang, *Adv. Mater.* **2017**, *29*, 1606134.
- [10] P. Horcajada, R. Gref, T. Baati, P. K. Allan, G. Maurin, P. Couvreur, G. Férey, R. E. Morris, C. Serre, *Chem. Rev.* **2012**, *112*, 1232–1268.
- [11] S. R. Batten, N. R. Champness, *Phil. Trans. R. Soc. A* **2017**, *375*, 20160032.
- [12] O. M. Yaghi, M. O'Keeffe, N. W. Ockwig, H. K. Chae, M. Eddaoudi, J. Kim, *Nature* **2003**, *423*, 705–714.
- [13] S. Yuan, L. Feng, K. Wang, J. Pang, M. Bosch, C. Lollar, Y. Sun, J. Qin, X. Yang, P. Zhang, Q. Wang, L. Zou, Y. Zhang, L. Zhang, Y. Fang, J. Li, H.-C. Zhou, *Adv. Mater.* **2018**, *30*, 1704303.
- [14] H. Li, K. Wang, Y. Sun, C. T. Lollar, J. Li, H.-C. Zhou, *Mater. Today* **2018**, *21*, 108–121.
- [15] J. Ren, H. W. Langmi, B. C. North, M. Mathe, *Int. J. Energy Res.* **2015**, *39*, 607–620.
- [16] M. Liu, J. Wu, H. Hou, *Chem. Eur. J.* **2019**, *25*, 2935–2948.
- [17] Y.-B. Huang, J. Liang, X.-S. Wang, R. Cao, *Chem. Soc. Rev.* **2017**, *46*, 126–157.
- [18] H.-Y. Li, S.-N. Zhao, S.-Q. Zang, J. Li, *Chem. Soc. Rev.* **2020**, *49*, 6364–6401.
- [19] L. E. Kreno, K. Leong, O. K. Farha, M. Allendorf, R. P. Van Duyne, J. T. Hupp, *Chem. Rev.* **2012**, *112*, 1105–1125.
- [20] L. S. Xie, G. Skorupskii, M. Dincă, *Chem. Rev.* **2020**, *120*, 8536–8580, <https://doi.org/10.1021/acs.chemrev.9b00766>.
- [21] S. K. Bhardwaj, N. Bhardwaj, R. Kaur, J. Mehta, A. L. Sharma, K.-H. Kim, A. Deep, *J. Mater. Chem. A* **2018**, *6*, 14992–15009.
- [22] M. Ding, X. Cai, H.-L. Jiang, *Chem. Sci.* **2019**, *10*, 10209.
- [23] B. Liu, K. Vikrant, K.-H. Kim, V. Kumar, S. K. Kailasa, *Environ. Sci.-Nano* **2020**, *7*, 1319–1347.
- [24] X. Liu, X. Wang, F. Kapteijn, *Chem. Rev.* **2020**, *120*, 8303–8377.
- [25] T. Devic, C. Serre, *Chem. Soc. Rev.* **2014**, *43*, 6097–6115.
- [26] R. G. Pearson, *J. Am. Chem. Soc.* **1963**, *85*, 3533–3539.
- [27] N. u Qadir, S. A. M. Said, H. M. Bahaidarah, *Microporous Mesoporous Mater.* **2015**, *201*, 61–90.
- [28] K. Leus, T. Bogaerts, J. D. Decker, H. Depauw, K. Hendrickx, H. Vrielinck, V. V. Speybroeck, P. V. D. Voort, *Microporous Mesoporous Mater.* **2016**, *226*, 110–116.
- [29] M. de J Velásquez-Hernández, R. Ricco, F. Carraro, F. T. Limpoco, M. Linares-Moreau, E. Leitner, H. Wilsche, J. Rattenberger, H. Schröttner, P. Frühwirth, E. M. Stadler, G. Gescheidt, H. Amenitsch, C. J. Doonan, P. Falcaro, *CrystEngComm* **2019**, *21*, 4538–4544.
- [30] M. A. Luzuriaga, C. E. Benjamin, M. W. Gaertner, H. Lee, F. C. Herbert, S. Mallick, J. J. Gassensmith, *Supramol. Chem.* **2019**, *31*, 485–490.
- [31] I. A. Lazaro, S. Haddad, S. Sacca, C. Orellana-Tavra, D. Fairen-Jimenez, R. S. Forgan, *Chem* **2017**, *2*, 561–578.
- [32] D. Bůžek, S. Adamec, K. Lang, J. Demel, *Inorg. Chem. Front.* **2021**, *8*, 720–734.
- [33] E. Bellido, M. Guillevis, T. Hidalgo, M. J. Santander-Ortega, C. Serre, P. Horcajada, *Langmuir* **2014**, *30*, 5911–5920.
- [34] T. Hidalgo, M. Giménez-Marqués, E. Bellido, J. Avila, M. C. Asensio, F. Salles, M. V. Lozano, M. Guillevis, R. Simón-Vázquez, A. González-Fernández, C. Serre, M. J. Alonso, P. Horcajada, *Sci. Rep.* **2017**, *7*, 43099.
- [35] M. R. C. Marques, R. Loebenberg, M. Almukainzi, *Dissolution Technol.* **2011**, *18*, 15–28.
- [36] J. W. Mauger, *Dissolution Technol.* **2017**, *24*, 38–51.
- [37] C. Orellana-Tavra, R. J. Marshall, E. F. Baxter, I. A. Lazaro, A. Tao, A. K. Cheetham, R. S. Forgan, D. Fairen-Jimenez, *J. Mater. Chem. B* **2016**, *4*, 7697–7707.
- [38] W. Cai, J. Wang, C. Chu, W. Chen, C. Wu, G. Liu, *Adv. Sci.* **2019**, *6*, 1801526.
- [39] X. Lin, Q. Hu, K. Jiang, Y. J. Cui, Y. Yang, G. D. Qian, *Microporous Mesoporous Mater.* **2017**, *249*, 55–60.
- [40] M. de J Velásquez-Hernández, M. Linares-Moreau, E. Astria, F. Carraro, M. Z. Alyami, N. M. Khashab, C. J. Sumby, C. J. Doonan, P. Falcaro, *Coord. Chem. Rev.* **2021**, *429*, 213651.

- [41] J. Fang, H. Nakamura, H. Maeda, *Adv. Drug Delivery Rev.* **2011**, *63*, 136–151.
- [42] I. F. Tannock, D. Rotin, *Cancer Res.* **1989**, *49*, 4373–4384.
- [43] S. Feng, X. Zhang, D. Shi, Z. Wang, *Front. Chem.* **2021**, *15*, 221–237.
- [44] Q. Wang, Y. Sun, S. Li, P. Zhang, Q. Yao, *RSC Adv.* **2020**, *10*, 37600–37620.
- [45] H. Zheng, Y. Zhang, L. Liu, W. Wan, P. Guo, A. M. Nyström, X. Zou, *J. Am. Chem. Soc.* **2016**, *138*, 962–968.
- [46] H. Ren, L. Zhang, J. An, T. Wang, L. Li, X. Si, L. He, X. Wu, C. Wang, Z. Su, *Chem. Commun.* **2014**, *50*, 1000–1002.
- [47] J. Zhuang, C. H. Kuo, L. Y. Chou, D. Y. Liu, E. Weerapana, C. K. Tsung, *ACS Nano* **2014**, *8*, 2812–2819.
- [48] C. Y. Sun, C. Qin, X. L. Wang, G. S. Yang, K. Z. Shao, Y. Q. Lan, Z. M. Su, P. Huang, C. G. Wang, E. B. Wang, *Dalton Trans.* **2012**, *41*, 6906–6909.
- [49] R. Ettlinger, N. Moreno, D. Volkmer, K. Kerl, H. Bunzen, *Chem. Eur. J.* **2019**, *25*, 13189–13196.
- [50] R. Ettlinger, N. Moreno, N. Ziolkowska, A. Ullrich, H.-A. Krug von Nidda, D. Jirak, K. Kerl, H. Bunzen, *Part. Part. Syst. Character.* **2020**, *37*, 2000185.
- [51] J. Schnabel, R. Ettlinger, H. Bunzen, *ChemNanoMat* **2020**, *6*, 1229–1236.
- [52] R. Ettlinger, M. Sönksen, M. Graf, N. Moreno, D. Denysenko, D. Volkmer, K. Kerl, H. Bunzen, *J. Mater. Chem. B* **2018**, *6*, 6481–6489.
- [53] Y. D. Zhu, S. P. Chen, H. Zhao, Y. Yang, X. Q. Chen, J. Sun, H. S. Fan, X. D. Zhang, *ACS Appl. Mater. Interfaces* **2016**, *8*, 34209–34217.
- [54] P. F. Gao, L. L. Zheng, L. J. Liang, X. X. Yang, Y. F. Li, C. Z. Huang, *J. Mater. Chem. B* **2013**, *1*, 3202–3208.
- [55] X. Zhu, J. Gu, Y. Wang, B. Li, Y. Li, W. Zhao, J. Shi, *Chem. Commun.* **2014**, *50*, 8779–8782.
- [56] Y. Yang, Q. Hu, Q. Zhang, K. Jiang, W. Lin, Y. Yang, Y. Cui, G. Qian, *Mol. Pharmaceutics* **2016**, *13*, 2782–2786.
- [57] W. Lin, Q. Hu, K. Jiang, Y. Yang, Y. Cui, G. Qian, *J. Solid State Chem.* **2016**, *237*, 307–312.
- [58] Y. Chen, P. Li, J. A. Modica, R. J. Drouot, O. K. Farha, *J. Am. Chem. Soc.* **2018**, *140*, 5678–5681.
- [59] B. DeCoste, G. W. Peterson, H. Jasuja, T. G. Glover, Y.-g. Huang, K. S. Walton, *J. Mater. Chem. A* **2013**, *1*, 5642–5650.
- [60] R. S. Forgan, *Dalton Trans.* **2019**, *48*, 9037–9042.
- [61] C. V. McGuire, R. S. Forgan, *Chem. Commun.* **2015**, *51*, 5199–5217.
- [62] S. B. van Witteloostuijn, S. L. Pederson, K. J. Jensen, *ChemMedChem* **2016**, *11*, 2474–2495.
- [63] C. Orellana-Tavra, E. F. Baxter, T. Tian, T. D. Bennett, N. K. H. Slater, A. K. Cheetham, D. Fairen-Jimenez, *Chem. Commun.* **2015**, *51*, 13878–13881.

Manuscript received: May 19, 2021
Accepted manuscript online: June 18, 2021
Version of record online: July 1, 2021